

Optimal Sensing Precision for Celestial Navigation Systems in Cislunar Space using LPV Framework

Eliot Nychka

Raktim Bhattacharya

Aerospace Engineering, Texas A&M University,
College Station, TX, 77843-3141.

Abstract—This paper introduces two innovative convex optimization formulations to simultaneously optimize the $\mathcal{H}_2/\mathcal{H}_\infty$ observer gain and sensing precision, and guarantee a specified estimation error bound for nonlinear systems in LPV form. Applied to the design of an onboard celestial navigation system for cislunar operations, these formulations demonstrate the ability to maintain accurate spacecraft positioning with minimal measurements and theoretical performance guarantees by design.

Keywords—LPV Systems, Convex Optimization, Navigation Systems, Robust Control

I. INTRODUCTION

The recent surge in interest toward cislunar space – the region within the gravitational spheres of influence of Earth and the Moon – is fueled by military and commercial motivations. The strategic significance of cislunar space lies in its potential to host assets for advanced surveillance and communication systems that exceed the capabilities within geostationary orbit, thus enhancing national security. From a commercial perspective, cislunar space represents a frontier of untapped potential, promising lucrative opportunities in areas such as resource extraction, space tourism, and as a launchpad for further solar system exploration. These prospects underscore the substantial economic implications of Cislunar development.

Space Domain Awareness (SDA) in cislunar space is crucial as activities within this region increase. The strategic and economic significance of cislunar space necessitates sophisticated SDA capabilities to ensure the safety of navigational operations and the integrity of space assets. Effective SDA in cislunar space involves comprehensive monitoring, tracking, and predictive analytics to manage space traffic, debris, and potential threats, which are essential for collision avoidance and operational security.

Recently, planar Earth-Moon resonant orbits have been proposed as a feasible strategy for comprehensive cislunar SDA (CSDA) [1]. Such a scenario is shown in Fig.1, where surveillance platforms (shown as black dots) move along a candidate resonant orbit in sufficient large numbers to ensure

necessary coverage, for example, to track a resident space object (RSO) shown in magenta.

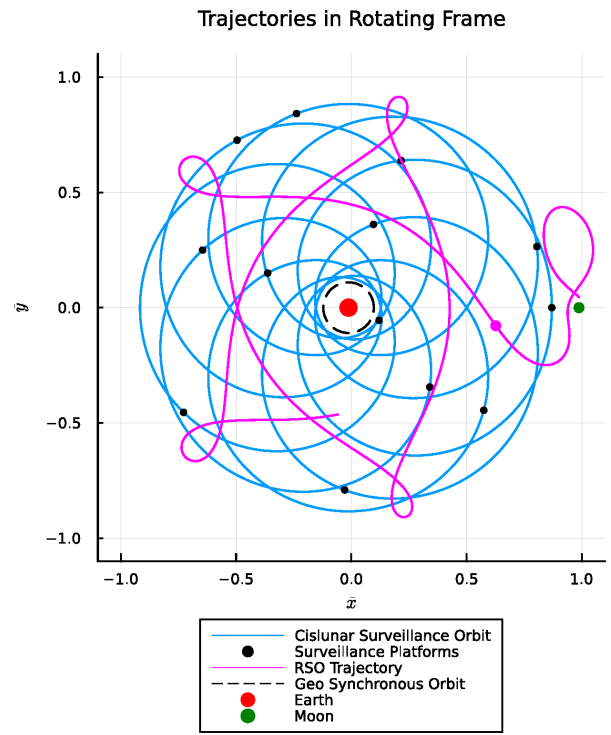


Figure 1: Earth-Moon resonant orbits in cislunar space for tracking resident space objects (RSOs).

The reliability of such surveillance systems depends on the ability of each surveillance agent to navigate robustly in the cislunar space, which is challenging due to the complex dynamic interaction between the Earth and the Moon and limited sensing abilities. The gravitational interactions between the Earth, Moon, and spacecraft lead to non-linear and chaotic dynamics, particularly in regions influenced by Earth's and Moon's gravity. Celestial navigation is a proven method in deep space and relies on observations of stars, the Sun, the Earth, and the Moon to determine the spacecraft's position and orientation. However, its application in cislunar space requires high precision in sensor technology and sophisticated algorithms robust to chaotic cislunar dynamics.

State-of-the-art celestial navigation systems for spacecraft use advanced algorithms and technologies to achieve accurate position and orientation estimates, essential for deep-space missions. These systems predominantly use star trackers and sextants to observe celestial bodies and employ sophisticated filtering techniques like the Extended Kalman Filter (EKF) and the Unscented Kalman Filter (UKF) to handle nonlinearities and uncertainties inherent in the system [2], [3]. Additionally, Particle Filters are implemented to manage non-Gaussian noise environments, providing robustness in complex scenarios [3]. Since these approaches are based on several approximations, e.g., linearization, Gaussian uncertainty models, and sample approximations, they do not provide global performance guarantees. The practical effectiveness in specific applications is often validated through experimental setups and simulations tailored to the particular characteristics of the system being modeled. Our recent work has developed an LPV (linear parameter varying) framework for developing celestial navigation systems for Cislunar applications [4] with guaranteed bounds on the estimator’s error in the $\mathcal{L}_\infty/\mathcal{L}_2$ sense.

The issue with these methods is that the sensor precision needs to be specified as input to the design, and the estimator’s accuracy depends on it. In celestial navigation systems designed for spacecraft, the configuration and quantity of sensors vary significantly based on mission objectives, spacecraft design, and the operational environment. Commonly incorporated sensors include multiple star trackers for reliable star positioning, which is essential for maintaining orientation. Sun and Earth sensors determine the spacecraft’s orientation relative to the Sun and Earth, providing vital data for orbits close to Earth. Inertial Measurement Units (IMUs), which consist of accelerometers and gyroscopes, are necessary for tracking changes in attitude and velocity. Magnetometers are often used in Earth orbit to measure magnetic fields, aiding in attitude control. Additional sensors like optical devices for detailed celestial observations and radio navigation systems for precise positioning using Earth-based or inter-satellite signals may also be included. The key challenge here is to determine the precision of these sensors to meet a given mission’s error budget. Often, unnecessarily high-precision sensors are used, resulting in expensive systems.

This paper addresses the challenge by simultaneously optimizing sensor precision and synthesizing the corresponding estimator that ensures user-specified estimation accuracy. We address this issue by expanding the LPV formulation presented in [4] to include sensor precision optimization. To the best of our knowledge, this is the first paper that addresses this problem.

II. SPECIFIC CONTRIBUTIONS

The primary contributions of this paper are two new convex optimization formulations to determine a nonlinear state estimator in LPV form and minimum sensing precision

that achieves a user-specified bound on estimation error. The results are presented for \mathcal{H}_2 and \mathcal{H}_∞ robust estimation framework and detailed in §III-C and §III-D.

III. PROBLEM FORMULATION

A. Brief Overview of LPV Systems

Linear Parameter Varying (LPV) [5], [6] control systems represent an advanced approach in control theory for handling nonlinear systems by employing a family of linear controllers. These controllers are scheduled based on varying parameters that are measurable in real time. The LPV framework extends the gain scheduling approach, which traditionally involves designing controllers at various operating points and interpolating between them as system parameters change. The interpolated controller does not have theoretical guarantees. However, the LPV framework provides theoretical guarantees since the design accounts for parameter variations. Several methodologies exist for designing LPV controllers, including *linear fractional transformations (LFT)*, *single quadratic Lyapunov function (SQLF)*, and *parameter dependent quadratic Lyapunov function (PDQLF)*. These methodologies reformulate control design problems into convex optimization problems involving linear matrix inequalities (LMIs) [7], [8]. The main challenge is representing the nonlinear system as a linear parameter-varying system. For example, a nonlinear system $\dot{x} = x^3$ can be written as $\dot{x} = A(\rho)x$, where $A(\rho) = \rho$ with $\rho(t) := x^2(t)$. When LPV models are affine in the parameter, i.e., $A(\rho) = A_0 + A_1\rho$, the constraints to guarantee performance for all variation in $\rho(t)$ are simpler. It is assumed $\rho(t)$ is in a convex polytope, and guarantees are established with constraints defined on the vertices of the polytope. If the dependence on $\rho(t)$ is nonlinear, randomized algorithms are often employed with probabilistic guarantees [9], [10]. Often, additional parameters are introduced to force an affine structure, resulting in many parameters. The computational burden increases with problem size and is dominated by the worst-case complexity of LMIs are $\mathcal{O}(n^6)$, where n is the problem size. Also, restricting $\rho(t)$ in a closed set is often not trivial. Besides these limitations, the LPV framework has been quite successful, particularly in the aerospace industry [11]–[14].

B. LPV Observer Design

We consider the following LPV system

$$\dot{x}(t) = A(\rho)x(t) + b(\rho) + B_w(\rho)w(t), \quad (1a)$$

$$y(t) = C(\rho)x(t) + d(\rho) + D_w(\rho)w(t), \quad (1b)$$

$$z(t) = C_zx(t), \quad (1c)$$

where $x \in \mathbb{R}^{N_x}$, $y \in \mathbb{R}^{N_y}$ are respectively the state vector, the vector of measured outputs, and the output vector of interest, and $\rho \in \mathbb{R}^{N_\rho}$ is the parameter on which the dynamics

is scheduled. Also, $w \in \mathbb{R}^{N_w}$ is the vector of the exogenous signals and is noted as:

$$w(t) = \begin{bmatrix} d(t) \\ n(t) \end{bmatrix}, \quad (2)$$

where $d \in \mathbb{R}^{N_d}$ is the disturbance and $n \in \mathbb{R}^{N_y}$ is the measurement noise.

Remark. Note that the dynamics in (1) has the terms $b(\rho)$ and $d(\rho)$, which admits nonlinear systems that cannot be expressed as LPV but as affine parameter varying systems. The nonlinear system in the classical Cislunar CR3BP (circular restricted three-body problem) is one such system.

The full-order nonlinear state observer in LPV form for the system (1) is given by

$$\dot{\hat{x}}(t) = \left(A(\rho) + LC_y(\rho) \right) \hat{x}(t) - Ly(t) + \left(b(\rho) + Ld(\rho) \right), \quad (3a)$$

$$\hat{z} = C_z \hat{x}(t), \quad (3b)$$

where $\hat{x} \in \mathbb{R}^{N_z}$ is the estimated state vector, $\hat{x} \in \mathbb{R}^{N_z}$ is the estimate of the vector of interest, and $L \in \mathbb{R}^{N_z \times N_y}$ is the observer gain. The error vector is defined as

$$e(t) = x(t) - \hat{x}(t), \text{ and } \epsilon(t) = z(t) - \hat{z}(t). \quad (4)$$

Remark. Note that the estimator dynamics in (3) is different from the conventional formulation as it has the $b(\rho)$ and $d(\rho)$ terms to account for the affine form of the LPV system in (1).

The error dynamics is then given by

$$\dot{e}(t) = (A(\rho) + LC_y(\rho))e(t) + ([B_d(\rho)S_d \ 0] + L [D_d(\rho)S_d \ S_n])\bar{w}(t), \quad (5a)$$

$$\epsilon(t) = C_z e(t), \quad (5b)$$

where \bar{w} is the normalized exogeneous input with $\|\bar{w}\|_2 = 1$. The variables S_d and S_n scale the inputs to the physical space. In particular, S_n scales the sensor noise, which is an optimization variable in the subsequent formulation.

The transfer function from $\bar{w}(t)$ to error $\epsilon(t)$ is then given by,

$$G_{\bar{w} \rightarrow \epsilon}(s, \rho) := C_z (sI_{N_x} - A(\rho) - LC_z(\rho))^{-1} (B_{\bar{w}} + LD_{\bar{w}}), \quad (6)$$

where $B_{\bar{w}}(\rho) = [B_d(\rho)S_d \ 0]$ and $D_{\bar{w}}(\rho) = [B_d(\rho)S_d \ S_n]$.

We are interested in determining the gain L , such that $\|G_{\bar{w} \rightarrow \epsilon}(s, \rho)\|_p < \gamma$ for $p = 2, \infty$, while maximizing the noise in the sensor. The sensor noise $n(t) := S_n \bar{n}(t)$, where $\|\bar{n}(t)\|_2 = 1$ and $S_n := \mathbf{diag}(\kappa_1 \ \cdots \ \kappa_{N_y})$, with $\kappa_i := 1/\|n_i(t)\|_2$ defined as the precision of the i^{th} sensor. We also define $\beta_i := \kappa_i^2$, and the corresponding vector $\beta := [\beta_1 \ \cdots \ \beta_{N_y}]^T$. It turns out that the problem is convex in β for $p = 2, \infty$, as shown in the next two sections.

C. Optimal Sensing Precision for \mathcal{H}_2 -LPV Observers

Theorem 1. The optimal sensing precision and observer gain for an LPV estimator with $\|G_{\bar{w} \rightarrow \epsilon}(s, \rho)\|_2 < \gamma$ is given by the convex optimization problem

$$\left. \begin{aligned} & \min_{Y, Q > 0, X > 0, \beta > 0} \|\beta\|_p \text{ such that,} \\ & M_{11} = XA(\rho) + YC_y(\rho) \\ & \quad + (XA(\rho) + YC_y(\rho))^T, \\ & M_{12} = XB_d(\rho)S_d + YCD_d(\rho)S_d, \\ & \begin{bmatrix} M_{11} & M_{12} & Y \\ M_{12}^T & -I_{N_d} & 0 \\ Y^T & 0 & -\mathbf{diag}(\beta) \end{bmatrix} < 0, \\ & \begin{bmatrix} -Q & C_z(\rho) \\ C_z^T(\rho) & -X \end{bmatrix} < 0, \\ & \text{trace}(Q) < \gamma^2 \end{aligned} \right\} \quad (7)$$

where the optimal sensing precision $\kappa_i = \sqrt{\beta_i}$, and $L := X^{-1}Y$.

Proof. The condition $\|G_{\bar{w} \rightarrow \epsilon}(s)\|_2 < \gamma$ is equivalent to the existence of a symmetric matrix $P > 0$ such that [15]

$$(A + LC_y(\rho)P + P(A + LC_y(\rho))^T + (B_{\bar{w}}(\rho) + LB_{\bar{w}}(\rho))(B_{\bar{w}}(\rho) + LB_{\bar{w}}(\rho))^T) < 0 \quad (8a)$$

$$\text{trace}(C_z(\rho)PC_z^T(\rho)) < \gamma \quad (8b)$$

Pre- and post-multiplying 8a by P^{-1} gives

$$P^{-1}(A + LC_y(\rho) + (A + LC_y(\rho))^T P^{-1} + P^{-1}(B_{\bar{w}}(\rho) + LB_{\bar{w}}(\rho))(B_{\bar{w}}(\rho) + LB_{\bar{w}}(\rho))^T P^{-1}) < 0 \quad (9)$$

Letting $X := P^{-1}$ and $Y := XL$ in the previous equation to get

$$(XA + YC_y(\rho) + (XA + YC_y(\rho))^T + (XB_{\bar{w}}(\rho) + YB_{\bar{w}}(\rho))(XB_{\bar{w}}(\rho) + YB_{\bar{w}}(\rho))^T) < 0 \quad (10)$$

Then using the definition of $B_{\bar{w}}(\rho)$ and $D_{\bar{w}}(\rho)$, and $M_{11} := (XA + YC_y(\rho) + (XA + YC_y(\rho))^T)$, and defining $M_{12} := XB_d(\rho)S_d + YCD_d(\rho)S_d$ the inequality in (10) can be written as

$$M_{11} + [M_{12} \ YS_n] \begin{bmatrix} M_{12}^T \\ S_n^T Y^T \end{bmatrix} < 0, \text{ or}$$

$$M_{11} + [M_{12} \ YS_n] \begin{bmatrix} I_{N_d} & 0 \\ 0 & S_n S_n^T \end{bmatrix} \begin{bmatrix} M_{12}^T \\ S_n^T Y^T \end{bmatrix} < 0.$$

Applying Schur's complement and substituting $\beta_i := \kappa_i^2$ the inequality becomes,

$$\begin{bmatrix} M_{11} & M_{12} & Y \\ M_{12}^T & -I_{N_d} & 0 \\ Y^T & 0 & -\mathbf{diag}(\beta) \end{bmatrix} < 0, \quad (11)$$

Now applying Schur's complement to the inequality (8b), we get $C_z(\rho)PC_z^T(\rho) - Q < 0$ and $\text{trace}(Q) < \gamma^2$, for $Q > 0$. Finally, using Schur's complement lemma and substituting $P^{-1} = X$ we get

$$\begin{bmatrix} -Q & C_z(\rho) \\ C_z^T(\rho) & -X \end{bmatrix} < 0, \text{trace}(Q) < \gamma^2. \quad (12)$$

Therefore the convex optimization formulation is given by

$$\min_{Y, Q > 0, X > 0, \beta > 0}, \text{subject to (11) and (12)}$$

D. Optimal Sensing Precision for \mathcal{H}_∞ -LPV Observers

Theorem 2. *The optimal sensing precision and observer gain for an LPV estimator with $\|G_{\bar{w} \rightarrow \epsilon}(s, \rho)\|_\infty < \gamma$ is given by the convex optimization problem*

$$\left. \begin{array}{l} \min_{Y, Q > 0, X > 0, \beta > 0} \|\beta\|_p \text{ such that,} \\ M_{11}(\rho) = \mathbf{sym}(XA(\rho) + YC_y(\rho)), \\ M_{12}(\rho) = XB_d(\rho)S_d + YCD_d(\rho)S_d, \\ \left[\begin{array}{cccc} M_{11}(\rho) & M_{12}(\rho) & C_z^T(\rho) & Y \\ M_{12}^T(\rho) & -\gamma^2 I_{N_d} & 0 & 0 \\ C_z(\rho) & 0 & -I_{N_z} & 0 \\ Y^T & 0 & 0 & -\gamma^2 \mathbf{diag}(\beta) \end{array} \right] < 0, \end{array} \right\} \quad (13)$$

where the optimal precision is given by $\kappa_i = \sqrt{\beta_i/\gamma}$, and $L = X^{-1}Y$.

Proof. The condition $\|G_{\bar{w} \rightarrow \epsilon}(s, \rho)\|_\infty < \gamma$ is equivalent to a symmetric matrix $X > 0$ such that [15]

$$\left[\begin{array}{cc} \mathbf{sym}(XA(\rho) + XLC_y(\rho) \\ + C_z(\rho)C_z(\rho)^T & X(B_{\bar{w}}(\rho) + LD_{\bar{w}}(\rho)) \\ (B_{\bar{w}}(\rho) + LD_{\bar{w}}(\rho))^T X & -\gamma^2 I_{(N_d + N_y)}. \end{array} \right] < 0 \quad (14)$$

Defining $Y := XL$ and the 14 equation becomes

$$\left[\begin{array}{cc} \mathbf{sym}(XA(\rho) + XLC_y(\rho) \\ + C_z(\rho)C_z(\rho)^T & XB_{\bar{w}}(\rho) + YD_{\bar{w}}(\rho) \\ (XB_{\bar{w}}(\rho) + YD_{\bar{w}}(\rho))^T X & -\gamma^2 I_{(N_d + N_y)}, \end{array} \right] < 0 \quad (15)$$

where $\mathbf{sym}(\cdot) := (\cdot) + (\cdot)^T$.

Using Schur's complement, the inequality can be rewritten as

$$\begin{aligned} & \mathbf{sym}(XA(\rho) + YC_y(\rho)) + C_z^T(\rho)C_z(\rho) \\ & + \gamma^{-2}(XB_{\bar{w}}(\rho) + YD_{\bar{w}}(\rho))(XB_{\bar{w}}(\rho) + YD_{\bar{w}}(\rho))^T < 0 \end{aligned} \quad (16)$$

Using the definitions of $B_{\bar{w}}(\rho)$ and $D_{\bar{w}}(\rho)$ as well as defining $M_{11}(\rho) := \mathbf{sym}(XA(\rho) + YC_y(\rho))$, and $M_{12}(\rho) := XB_d(\rho)S_d + YB_d(\rho)S_d$, the inequality 16 becomes

$$M_{11}(\rho) + [M_{12}(\rho) \quad C_z^T(\rho) \quad Y] R \begin{bmatrix} M_{12}^T(\rho) \\ C_z(\rho) \\ Y^T \end{bmatrix} < 0. \quad (17)$$

Where $R := \mathbf{diag}(\gamma^{-2}I_{N_d}, I_{N_z}, \gamma^{-2}S_n S_n^T)$. we can then use the fact $\kappa^2 = \beta = S_n S_n^T$ and then use Schur's complement to get.

$$\left[\begin{array}{cccc} M_{11}(\rho) & M_{12}(\rho) & C_z^T(\rho) & Y \\ M_{12}^T(\rho) & -\gamma^2 I_{N_d} & 0 & 0 \\ C_z(\rho) & 0 & -I_{N_z} & 0 \\ Y^T & 0 & 0 & -\gamma^2 \mathbf{diag}(\beta) \end{array} \right] < 0. \quad (18)$$

Therefore the convex optimization formulation in 18 is the same as the one shown in 13, i.e.,

$$\min_{Y, Q > 0, X > 0, \beta > 0}, \text{subject to 18}$$

Remark. *The cost function in the above optimization problems is given by $\|\beta\|_p$. If $p = 1$, the optimal solution will be sparse if it exists. This may be useful if a sensor selection problem is solved, since sensors with zero precisions can be eliminated from the design.*

Remark. *The LMIs in the above optimization problems are affine functions of ρ . We assume that ρ is in a convex polytope. Enforcing the LMIs at the vertices of the polytope guarantees that the LMIs are satisfied for all ρ in the convex polytope [16].*

IV. RESULTS

A. Representation of Cislunar Dynamics in LPV Form

We consider the classical circular restricted three-body problem (CR3BP). This simplified celestial mechanics model describes the motion of a small body under the gravitational influence of two larger bodies that are orbiting each other in circular orbits. The two larger bodies, called the primary bodies, are usually much more massive than the small body and are assumed to follow fixed circular orbits around their common center of mass due to their gravitational interaction. The small body, which is considered to have negligible mass compared to the other two, does not affect their motion. In the Cislunar case, the larger bodies are the Earth and the Moon, and the smaller body is the spacecraft or any resident space object.

The equations of motion for the CR3BP are,

$$\ddot{\bar{x}} - 2\dot{\bar{y}} - \bar{x} = -\frac{1 - \pi_2}{\sigma^3}(\bar{x} + \pi_2) - \frac{\pi_2}{\psi^3}(\bar{x} - 1 + \pi_2), \quad (19)$$

$$\ddot{\bar{y}} + 2\dot{\bar{x}} - \bar{y} = -\frac{1 - \pi_2}{\sigma^3}\bar{y} - \frac{\pi_2}{\psi^3}\bar{y}, \quad (20)$$

$$\ddot{\bar{z}} = -\frac{1 - \pi_2}{\sigma^3}\bar{z} - \frac{\pi_2}{\psi^3}\bar{z}, \quad (21)$$

where

$$\pi_1 = \frac{m_1}{m_1 + m_2}, \quad \pi_2 = \frac{m_2}{m_1 + m_2}, \quad (22)$$

and

$$\begin{aligned} \sigma & := \|\sigma\|_2, \text{ where } \sigma = \begin{bmatrix} \mathbf{r}_{13} \\ r_{12} \end{bmatrix} = (\bar{x} + \pi_2)\hat{i} + \bar{y}\hat{j} + \bar{z}\hat{k}, \text{ and} \\ \psi & := \|\psi\|_2, \text{ where } \psi = \begin{bmatrix} \mathbf{r}_{23} \\ r_{12} \end{bmatrix} = (\bar{x} + \pi_2 - 1)\hat{i} + \bar{y}\hat{j} + \bar{z}\hat{k}, \end{aligned}$$

and r_{12} is the distance between the Earth and the Moon. The coordinates are normalized with respect to r_{12} , i.e., \bar{x} , \bar{y} , \bar{z} are $\frac{x}{r_{12}}$, $\frac{y}{r_{12}}$, $\frac{z}{r_{12}}$ respectively. We define parameters $\rho := [\rho_1, \dots, \rho_6]^T$ with

$$\begin{aligned} \rho_1 &= \frac{1}{\sigma^3}, & \rho_2 &= \frac{1}{\psi^3}, & \rho_3 &= \frac{1}{\sigma}, \\ \rho_4 &= \frac{1}{\psi}, & \rho_5 &= \bar{x}, & \rho_6 &= \bar{y}. \end{aligned}$$

The nonlinear equations in (21) can now be written as the following LPV system (with affine dependence on the parameters),

$$\begin{aligned} \begin{bmatrix} \dot{\bar{x}} \\ \dot{\bar{y}} \\ \ddot{\bar{x}} \\ \ddot{\bar{y}} \end{bmatrix} &= \begin{bmatrix} 0 & 0 & 1 & 0 \\ 0 & 0 & 0 & 1 \\ \rho_1(\pi_2 - 1) + 1 & 0 & 0 & 2 \\ 0 & \rho_1(\pi_2 - 1) + 1 & -2 & 0 \end{bmatrix} \begin{bmatrix} \bar{x} \\ \bar{y} \\ \dot{\bar{x}} \\ \dot{\bar{y}} \end{bmatrix} \\ &+ \begin{bmatrix} 0 & 0 & 0 & 0 \\ 0 & 0 & 0 & 0 \\ -\rho_2\pi_2 & 0 & 0 & 0 \\ 0 & -\rho_2\pi_2 & 0 & 0 \end{bmatrix} \begin{bmatrix} \bar{x} \\ \bar{y} \\ \dot{\bar{x}} \\ \dot{\bar{y}} \end{bmatrix} \\ &+ \begin{bmatrix} 0 \\ 0 \\ \rho_1\pi_2 + \rho_2(\pi_2 - 1) \\ 0 \end{bmatrix}. \end{aligned} \quad (23)$$

The sensor model is defined as

$$\begin{aligned} \begin{bmatrix} \sin \theta_1 \\ \cos \theta_1 \\ \sin \theta_2 \\ \cos \theta_2 \\ r_{13}^2 \\ r_{23}^2 \end{bmatrix} &= \begin{bmatrix} 0 & \rho_3 \\ \rho_3 & 0 \\ 0 & \rho_4 \\ -\rho_4 & 0 \\ \rho_5 + 2\pi_2 & \rho_6 \\ \rho_5 + 2\pi_2 - 2 & \rho_6 \end{bmatrix} \begin{bmatrix} \bar{x} \\ \bar{y} \end{bmatrix} \\ &+ \begin{bmatrix} 0 \\ \rho_3\pi_2 \\ 0 \\ (-\rho_4(\pi_2 - 1)) \\ \pi_2^2 \\ (\pi_2 - 1)^2 \end{bmatrix}, \end{aligned} \quad (24)$$

to ensure that the model is affine in the parameters. This

leads to the affine forms of each state space matrix

$$\begin{aligned} A(\rho) &= \begin{bmatrix} 0 & 0 & 1 & 0 \\ 0 & 0 & 0 & 1 \\ \rho_1(\pi_2 - 1) & 0 & 0 & 2 \\ -\rho_2\pi_2 + 1 & \rho_1(\pi_2 - 1) & 0 & 0 \\ 0 & -\rho_2\pi_2 + 1 & -2 & 0 \end{bmatrix}, \\ b(\rho) &= \begin{bmatrix} 0 \\ 0 \\ \rho_1\pi_2 + \rho_2(\pi_2 - 1) \\ 0 \end{bmatrix}, d(\rho) = \begin{bmatrix} 0 \\ \rho_3 \\ 0 \\ -\rho_4 \\ \rho_5 + 2\pi_2 \\ \rho_5 + 2\pi_2 - 2 \end{bmatrix}, \\ C_y(\rho) &= \begin{bmatrix} 0 & \rho_3 & 0 & 0 \\ \rho_3 & 0 & 0 & 0 \\ 0 & \rho_4 & 0 & 0 \\ -\rho_4 & 0 & 0 & 0 \\ \rho_5 + 2\pi_2 & \rho_6 & 0 & 0 \\ \rho_5 + 2\pi_2 - 2 & \rho_6 & 0 & 0 \end{bmatrix}, C_z = \begin{bmatrix} 1 & 0 & 0 & 0 \\ 0 & 1 & 0 & 0 \end{bmatrix}. \end{aligned} \quad (25)$$

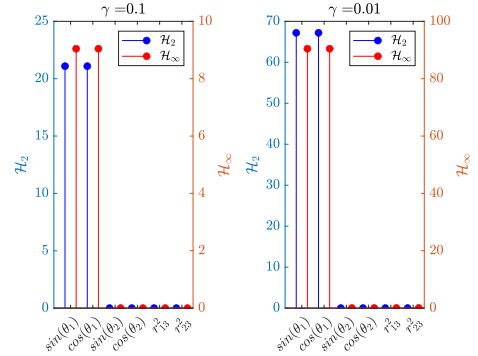


Figure 2: Optimal sensing precision κ .

B. Simulation Results

Utilizing the formulation in theorems 1 and 2 we get the sensing precisions shown in Fig.2. We observe that the algorithm only requires sensors that provide $\sin(\theta_1)$ and $\cos(\theta_1)$. In practice, however, θ_1 is measured from optical systems. Noting that the precision for $\sin(\theta_1)$ and $\cos(\theta_1)$ are identical, we can use either to compute the allowable noise in θ_1 , which can be determined from

$$\begin{aligned} \theta_1 &= \sin^{-1}\left(\frac{1}{\kappa_1}\right), \text{ or} \\ \theta_1 &= \frac{\pi}{2} - \cos^{-1}\left(\frac{1}{\kappa_2}\right). \end{aligned} \quad (26)$$

For a $\gamma = 0.1$, the maximum sensor noise level that the system can take was found to be around 2.6° for \mathcal{H}_2 and 6.3° for \mathcal{H}_∞ . Plotting the two cases at 2.6° of noise as shown in Fig.3 and Fig.4. Since the \mathcal{H}_2 formulation bounds the \mathcal{L}_∞ of the error, the state estimates in Fig.3 has less oscillations

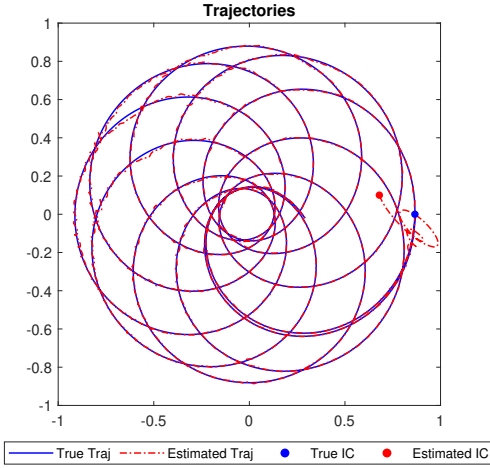


Figure 3: Trajectory and \mathcal{H}_2 Observation with 2.6° of Noise

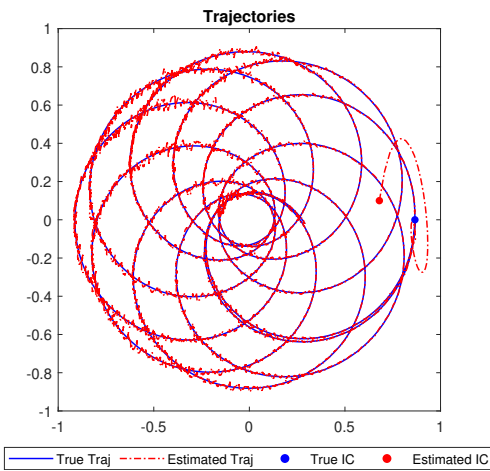


Figure 4: Trajectory and \mathcal{H}_∞ Observation with 2.6° of Noise

about the true values. The \mathcal{H}_∞ formulation bounds the \mathcal{L}_2 of the error, and therefore the state estimates in Fig.4 is more oscillatory.

The simulations start with significant errors in the initial state estimate. However, the algorithms are able to quickly converge to the neighbourhood of the true solution, which is significant given that the Cislunar dynamics is chaotic.

V. CONCLUSIONS

In this paper, we presented two innovative convex optimization formulations that simultaneously optimize the $\mathcal{H}_2/\mathcal{H}_\infty$ observer gain and the precision of sensing, guaranteeing a user-specified bound on the estimation error for nonlinear systems modeled as LPV systems.

These formulations were applied to the design of an on-board celestial navigation system for cislunar operations. The performance of these methods was confirmed by their ability to accurately predict the position of a spacecraft with minimal sensing. However, the current formulations do not account for sensing occlusions, which may require the integration

of additional sensors. The precision of sensing defined by our formulations can guide the design and production of sensing hardware, potentially leading to optimized hardware configurations.

In summary, the algorithms formulated in this study offer a robust framework for designing nonlinear state observers in LPV format. These observers are equipped with minimal sensing requirements and are backed by theoretical performance assurances, eliminating the dependence on empirical validation.

VI. ACKNOWLEDGMENT

This work is supported by AFOSR grant FA9550-22-1-0539 with Dr. Erik Blasch as the program director, and the Wheeler Graduate Fellowship.

REFERENCES

- [1] C. Frueh, K. Howell, K. DeMars, S. Bhadauria, and M. Gupta, "Cislunar space traffic management: Surveillance through earth-moon resonance orbits," in *8th European Conference on Space Debris*, vol. 8, 2021.
- [2] X. Ning and J. Fang, "An autonomous celestial navigation method for leo satellite based on unscented kalman filter and information fusion," *Aerospace science and Technology*, vol. 11, no. 2-3, pp. 222–228, 2007.
- [3] —, "Spacecraft autonomous navigation using unscented particle filter-based celestial/doppler information fusion," *Measurement Science and Technology*, vol. 19, no. 9, p. 095203, 2008.
- [4] E. Nychka and R. Bhattacharya, "Cislunar state estimation in the $\mathcal{H}_2/\mathcal{H}_\infty$ framework with linear parameter varying (lpv) models," *submitted AIAA Journal of Guidance, Control, and Dynamics*, 2024.
- [5] J. S. Shamma and M. Athans, "Analysis of gain scheduled control for nonlinear plants," *IEEE Transactions on Automatic Control*, vol. 35, no. 8, pp. 898–907, 1990.
- [6] J. S. Shamma, "An overview of lpv systems," *Control of linear parameter varying systems with applications*, pp. 3–26, 2012.
- [7] L. El Ghaoui and S.-I. Niculescu, *Advances in linear matrix inequality methods in control*. SIAM, 2000.
- [8] J. W. Helton and V. Vinnikov, "Linear matrix inequality representation of sets," *Communications on Pure and Applied Mathematics: A Journal Issued by the Courant Institute of Mathematical Sciences*, vol. 60, no. 5, pp. 654–674, 2007.
- [9] R. Tempo, G. Calafiore, F. Dabbene *et al.*, *Randomized algorithms for analysis and control of uncertain systems: with applications*. Springer, 2013, vol. 7.
- [10] Y. Fujisaki, F. Dabbene, and R. Tempo, "Probabilistic design of lpv control systems," *Automatica*, vol. 39, no. 8, pp. 1323–1337, 2003.
- [11] S. Ganguli, A. Marcos, and G. Balas, "Reconfigurable lpv control design for boeing 747-100/200 longitudinal axis," in *Proceedings of the 2002 American control conference (IEEE cat. no. CH37301)*, vol. 5. IEEE, 2002, pp. 3612–3617.
- [12] G. J. Balas, "Linear, parameter-varying control and its application to aerospace systems," in *ICAS congress proceedings*, 2002, pp. 541–1.
- [13] W. Gilbert, D. Henrion, J. Bernussou, and D. Boyer, "Polynomial lpv synthesis applied to turbofan engines," *Control engineering practice*, vol. 18, no. 9, pp. 1077–1083, 2010.
- [14] A. Marcos and S. Bannani, "Lpv modeling, analysis and design in space systems: Rationale, objectives and limitations," in *AIAA guidance, navigation, and control conference*, 2009, p. 5633.
- [15] V. M. Deshpande and R. Bhattacharya, "Sparse sensing and optimal precision: An integrated framework for $\mathcal{H}_2/\mathcal{H}_\infty$ optimal observer design," *IEEE Control Systems Letters*, vol. 5, no. 2, pp. 481–486, 2021.
- [16] P. Apkarian, P. Gahinet, and G. Becker, "Self-scheduled \mathcal{H}_∞ control of linear parameter-varying systems: a design example," *Automatica*, vol. 31, no. 9, pp. 1251–1261, 1995.